Triggered emission of indistinguishable photons from an organic dye molecule

Pietro Lombardi, Maja Colautti, Rocco Duquennoy, et al.

COLLECTIONS

Paper published as part of the special topic on Non-Classical Light Emitters and Single-Photon Detectors

View Online   Export Citation   CrossMark

ARTICLES YOU MAY BE INTERESTED IN

Invited Review Article: Single-photon sources and detectors
Review of Scientific Instruments **82**, 071101 (2011); https://doi.org/10.1063/1.3610677

Progress in quantum-dot single photon sources for quantum information technologies: A broad spectrum overview
Applied Physics Reviews **7**, 021309 (2020); https://doi.org/10.1063/5.0010193

A bright source of telecom single photons based on quantum frequency conversion
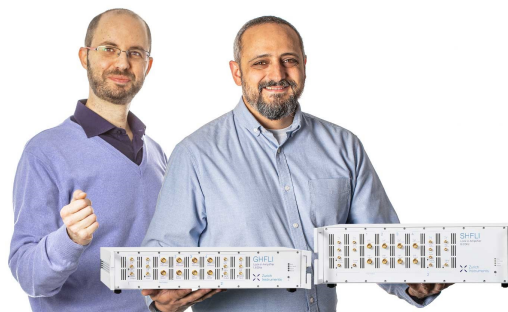Applied Physics Letters **118**, 174003 (2021); https://doi.org/10.1063/5.0045413

Triggered emission of indistinguishable photons from an organic dye molecule

View Online   Export Citation   CrossMark

Pietro Lombardi,[1,2,a] (iD) Maja Colautti,[1,2] Rocco Duquennoy,[3] Ghülam Murtaza,[1,2] (iD) Prosenjit Majumder,[1,2] and Costanza Toninelli[1,2,a] (iD)

AFFILIATIONS

[1]National Institute of Optics (CNR-INO), Largo Enrico Fermi 6, Firenze 50125, Italy
[2]European Laboratory for Non-Linear Spectroscopy (LENS), Via Nello Carrara 1, Sesto F.no 50019, Italy
[3]Dipartimento di Fisica e Astronomia, Universitá degli Studi di Firenze, Via G. Sansone 1, Sesto F.no 50019, Italy

Note: This paper is part of the APL Special Collection on Non-Classical Light Emitters and Single-Photon Detectors.
[a]Authors to whom correspondence should be addressed: pietroernesto.lombardi@ino.cnr.it and toninelli@lens.unifi.it

ABSTRACT

Single molecules in solid state matrices have been proposed as sources of single photon Fock states back 20 years ago. Their success in quantum optics and in many other research fields stems from the simple recipes used in the preparation of samples, with hundreds of nominally identical and isolated molecules. Main challenges as of today for their application in photonic quantum technologies are the optimization of light extraction and the on-demand emission of indistinguishable photons. We here present Hong–Ou–Mandel (HOM) experiments with photons emitted by a single molecule of dibenzoterrylene in an anthracene nanocrystal at 3 K, under continuous wave and also pulsed excitation. A detailed theoretical model is applied, which relies on independent measurements for most experimental parameters, hence allowing for an analysis of the different contributions to the two-photon interference visibility, from residual dephasing to spectral filtering. A HOM interference visibility of more than 75% is reported, which, according to the model, is limited by the residual dephasing present at the operating temperature.

Two-particle interference is one of the most striking consequences of quantum physics. After the first seminal experiments with photons,[1–4] the effect has been demonstrated also for massive particles and quasi-particles such as electrons,[5,6] plasmons,[7,8] and atoms.[9,10] Glauber well captured this phenomenon intuitively within a generalized picture of interference, affecting all measurement outcomes which result from multiple indistinguishable stories.[11] Two-particle interference though does not have any classical counterpart, not even in the case of light.[12] Indeed two-photon interference (TPI) is at the heart of many quantum technologies (see Ref. 13), potentially outperforming classical computation schemes,[14,15] offering physics-protected information,[16] simulating highly complex physical systems,[17–19] and enhancing the sensitivity of precise measurements.[20,21] The so-called Hong–Ou–Mandel (HOM) interferometer, originally developed to measure small time shifts[2,3] nowadays reaching attosecond resolution,[22] is a well-known experimental scheme unveiling TPI. Essentially it consists of two single photon detectors at the output ports of a beam splitter (BS). Due to the bosonic nature of photons, in the case of two indistinguishable photons impinging separately on the BS ports,

interference forces them to coalesce at one of the outputs, suppressing the rate of simultaneous coincidences and hence yielding the two-photon path-entangled state[23] $\frac{1}{\sqrt{2}}(|2,0\rangle + |0,2\rangle)$. In order to enable effective quantum interference, the involved particles have to be prepared in the very same quantum state, so as to determine indistinguishability among different possible events with the same output state. It is also well established that quantum emitters in the solid state play a major role in the generation of single photons on a deterministic basis,[24] which is key to the preparation of more complex states of light[25,26] that are useful for many protocols in quantum technologies. However, the ability of such systems to provide photons in the same quantum state remains one of the most elusive requirements to meet, in particular in the sub-micrometric environment of integrated photonics.[27,28]

Single molecules of polyaromatic hydrocarbons (PAH) in suitable host matrices are known for emitting with high quantum efficiency in very narrow (few-tens-of-MHz wide) and stable zero phonon lines (ZPL). Molecular quantum emitters can also be integrated inside complex and hybrid photonic structures, yielding almost

100% collection efficiency,[29] 99% light extinction[30] and allowing for on-chip photon manipulation,[31,32] (for a complete review see, e.g., Ref. 33). Very promising results have been reported in HOM interference experiments with single photon streams, obtained from molecular emitters after continuous wave (CW) laser pumping,[34–37] including the case of photons emitted by remote molecules.[38] However, triggered single photon pulses appear necessary in any kind of logic operation with photons. In this work, we demonstrate that single, indistinguishable photons can be generated by single PAH molecules, triggered by the laser excitation pulses. Notably, the results are obtained for non-resonant pumping of the ZPL and without coupling to optical cavities. Hong–Ou–Mandel experiments are reported, based on triggered single photons from single dibenzoterrylene (DBT) molecules in anthracene nanocrystals.[39] Such molecular source is particularly suitable to isolate single emitters with respect to neighboring ones and to the background, even when a spectrally broad pulsed laser is employed in excitation. It also proves to be photostable over a timescale of at least one month. For this experiment, we employ the sample geometry already presented in Ref. 40, where nanocrystals are deposited on a gold mirror and then stabilized with a 200 nm-thick layer of Polyvinyl alcohol (PVA).

In order to model the outcome of the HOM measurements, we independently characterize also the multi-photon emission probability, the emission linewidth, the molecule lifetime, and the setup parameters. The model that is briefly outlined in the supplementary material correctly describes our data and suggests that the main limitation to the observed raw-data visibility is to be found in the residual dephasing observed at 3 K, which is currently our lowest temperature of operation. Upon cooling down to 1.4 K, an intrinsic wave-function overlap of up to 95% can be estimated.

In Fig. 1(a), the experimental setup used for characterization and for the HOM measurements is outlined. Single-molecule fluorescence is excited and collected in an epi-fluorescence microscope through a 0.7-N.A. objective, using either a tunable CW laser ($\lambda = 783.5$ nm) or a pulsed laser with central wavelength $\lambda = 766.0$ nm, adjustable repetition rate, and 50-ps long pulses (Picoquant LDH-D-FA-765L,
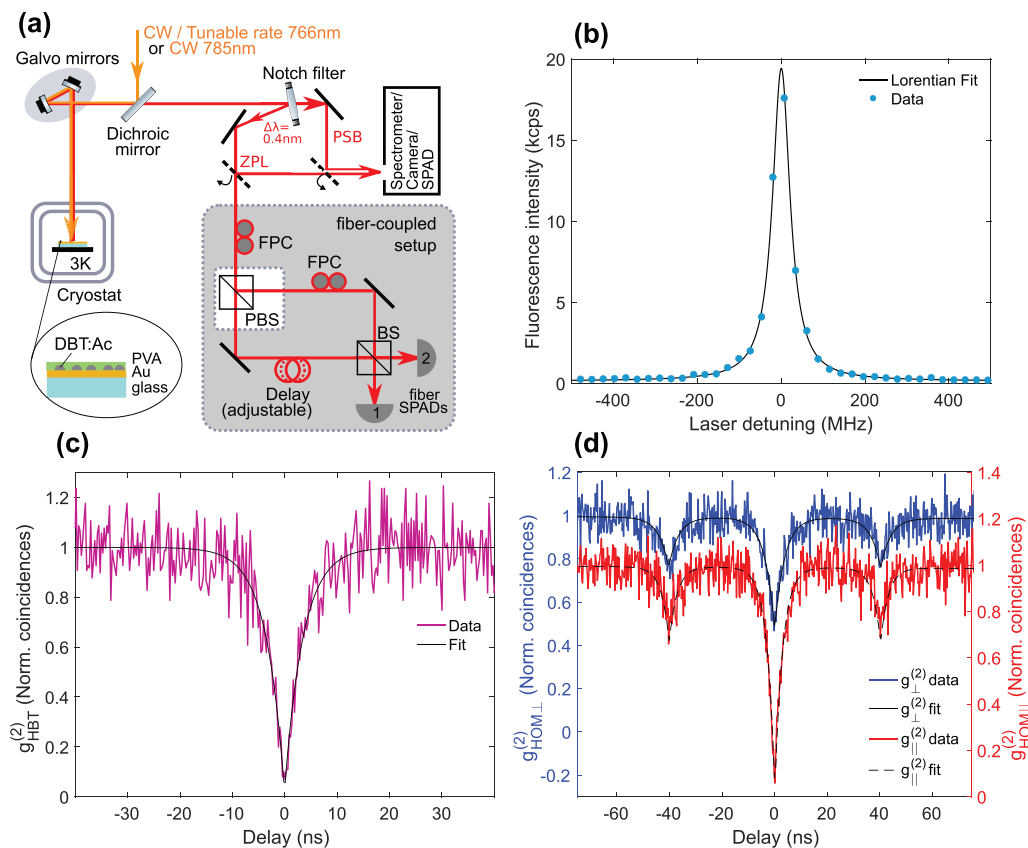

FIG. 1. (a) Sketch of the experimental setup. By means of a notch filter, the molecule emission collected in an epifluorescence-microscope configuration is separated in two parts containing the ZPL and the PSB. Both components can then be analyzed with a spectrometer and a free-space-coupled single photon avalanche diode (SPAD). The ZPL component can also enter the fibered circuit for probing purity and indistinguishability of the photon wave packet. (b) Excitation spectroscopy. Fluorescence intensity in the PSB as the frequency of a resonant laser is scanned across the ZPL. A Lorentzian fit to the data yields a FWHM of 55.1 ± 0.5 MHz. (c) Suppression of multi-photon emission events under CW operation. Histogram of the relative arrival time between the two SPADs in HBT configuration (no photons in the delay line arm). Solid line is a single exponential fit to the data, yielding $g^{(2)}(0) = 0.03 \pm 0.02$ and $\tau_1 = 3.5 \pm 0.2$ ns. (d) HOM results under CW operation. Histogram of the relative photon arrival times for parallel (red) and orthogonal (blue) polarizations are superimposed with shifted y-axis scale for clarity. Solid and dashed lines are fits to the data with expression (1). (c) and (d) are obtained integrating 100 kcps on each SPAD for 10 min (normalization level corresponding to around 250 coincidences; binning size 256 ps).

linewidth of about 0.3 nm), that can be operated in CW as well. A Longpass filter (Semrock LP02–785RE) is employed for rejection of the back-scattered pump light. The ZPL component at 783.5 nm is separated from the phonon sideband (PSB) exploiting a 0.4 nm-wide reflective Notch filter (OptiGrate BNF-785-OD4–12.5M) and coupled into a single-mode fiber. In order to probe the indistinguishability of consecutively emitted photons, the photon stream is split in two by a polarizing beam splitter cube (PBS), with a fiber polarization control in front (FPC, Thorlabs FPC023). One of the paths is then delayed by $\Delta t \simeq 40$ ns (8 m-long fiber), much longer than the excited state lifetime ($\simeq 4$ ns), as required to avoid temporal correlations between the photons in the two arms. Quantum interference in the train of single photon pulses is then measured by an unbalanced fiber-based Mach–Zehnder interferometer (MZI). In particular, a FPC unit is added on one path to switch between parallel and orthogonal configuration, before the MZI is closed on a fibered 50/50 BS (Thorlabs TN785R5A2). The two output ports are finally connected to a couple of single photon counting modules (Excelitas SPCM-NIR-14, quantum efficiency 70%). According to semi-analytical simulations,[41] the collection efficiency at first lens for the sample under investigation (and N.A. limited to 0.7) is estimated to be around 25%. Concerning the optical apparatus, the transmission of the free-space part of the setup is about 40%, the fiber coupling efficiency amounts to 60%, and the transmission of the fiber circuit to the SPADs is about 70%, corresponding to an optical setup efficiency of 17% and an overall efficiency of about 3%. The temporal resolution of the whole electronic chain involved in the start–stop measurement is 230 ps (see below and also supplementary material for details). When one of the interferometer arms is blocked, the setup operates in the so-called Hanbury–Brown and Twiss[42] (HBT) configuration, allowing for the characterization of the photon statistics. Instead, when the photon flux is equally distributed on the two arms, we can probe the photon indistinguishability through HOM interference. In Figs. 1(c) and 1(d), the histogram of the inter-photon arrival times for small time delays, normalized to the background average value, is reported for photon streams collected in the HBT and HOM configuration, respectively (saturation parameter $s \simeq 0.2$). In both cases, the dataset well reproduces the second order correlation function $g^2(\tau)$, probing multi-photon emission probability and indistinguishability of the photon stream. From the best fit to the data in Fig. 1(c) with equation $g_{HBT}^{(2)}(\tau) = (1 - b * \exp(-|\tau|/\tau_{HBT}))$, we obtain $g_{HBT}^{(2)}(0) = 0.03 \pm 0.02$.

Moreover, the effect of non-classical interference is clearly visible in panel d around zero time delay, where the data set for parallel polarization is well below the one for photons which are made distinguishable in polarization, i.e., to say, orthogonal. The other two dips occurring Δt-away from the main one correspond to the suppressed probability of having two photons closer than the emitter lifetime, in the case of one photon being transmitted/reflected when the other is reflected/transmitted. From the best fit to this measurement with the following equation, derived from Ref. 43 in the low saturation regime

$$g_{HOM}^{(2)}(\tau) = 2|r|^2|t|^2 g(\tau) + \left[|t|^4 g(\tau - \Delta t) + |r|^4 g(\tau + \Delta t) \right]$$
$$\times (1 - V e^{-|\tau|/\tau_{\parallel}}), \qquad (1)$$

with $g(t) = g_{HBT}^{(2)}(t)$ and $V = 0$ for orthogonal polarizations, we deduce $\Delta t = 40.3 \pm 0.2$ ns and the unbalance between reflectance $|r|^2$ and transmittance $|t|^2$ of the second beam splitter to be

$|r|^2/|t|^2 = 1.10 \pm 0.07$. The latter estimation is in agreement with direct measurements implemented with laser light at 783.5 nm, from which we evaluate both the overall losses of the fiber connector + BS (0.06 ± 0.01), and $|r|^2$ and $|t|^2$ values to be 0.50 ± 0.01 and 0.44 ± 0.01, respectively. These parameters will be used in analyzing the data for pulsed excitation, as they can be considered unchanged.

The degree of coherence of the molecule emission can be estimated as $|g^{(1)}(0)|^2 = \frac{g_{\perp}^{(2)}(0) - g_{\parallel}^{(2)}(0)}{g_{\perp}^{(2)}(0)} = 0.89 \pm 0.06$. This value results compatible with an estimate of the first order coherence from the second order autocorrelation function measured in HBT configuration, following the relationship:[36] $|g^{(1)}(0)|^2 = 1 - 2g_{HBT}^{(2)}(0) = 0.94 \pm 0.04$. It is important to notice that such visibility corresponds to the post-selected photons colliding at the beam splitter within a time-window much smaller than the photon wave packet duration (in our case 256 ps and 4 ns, respectively). As such, it is effective only at the price of a reduced emitter brightness. In other words, suppressed coincidences at zero time delay are expected also in a HOM experiment with detuned sources or in the presence of dephasing, with spectral fluctuations smaller than the inverse of the overall setup temporal resolution.[38] A non-perfect visibility in the case of severe post-selection can be hence ascribed only to the detector time-jitter, or to optical misalignment of the setup. The HOM interference profile in CW operation still gives some insight about the indistinguishability of the considered photon stream. Indeed, while the minimum of the dip is related to suppression of multi-photon emission events and other technical aspects, the characteristic time of the exponential profile depends on the coherence of the emission.[36] In detail, we find from the fits that the timescale of the dip for parallel configuration is shorter ($\tau_{\parallel} = 2.7 \pm 0.2$ ns) than that for orthogonal polarization ($\tau_{\perp} = 3.6(5) \pm 0.3(0)$ ns) and in the HBT case of Fig. 1(c) ($\tau_{HBT} = 3.5 \pm 0.2$ ns). This mismatch is expected in the presence of pure dephasing and corresponds to an estimation of the coherence time of the emitter equal to $\tau_c = 2\tau_{\parallel} = 5.4 \pm 0.5$ ns. It is interesting to compare this value with the direct measurement of the ZPL linewidth obtained via excitation spectroscopy that means recording the fluorescence signal in the PSB as a function of the excitation laser frequency, scanning across the ZPL [see Fig. 1(b)]. Indeed, in the latter case a FWHM of the Lorentzian fit to data yields a value of $= 55.1 \pm 0.5$ MHz, compatible with the estimate from HOM interference yielding $FWHM = 1/(\pi\tau_c) = 59 \pm 10$ MHz. We can conclude that the system shows negligible spectral diffusion under CW pumping, as the two estimate for the dephasing broadening are consistent within the error bars, although sensitive to frequency fluctuations on very different time scales (40 ns in the HOM measurements and seconds-long integration time for the excitation spectroscopy).

A more direct estimate of the photon wave packet overlap can be obtained addressing with laser pulses the molecule previously characterized in CW. First the fluorescence lifetime is measured, recording the histogram of the photon arrival times with respect to the laser excitation pulse. A typical dataset is reported in Fig. 2(c) and from the best fit with a single exponential decay, a lifetime $\tau_1 = 4.01 \pm 0.01$ ns is obtained, with uncertainty given by the standard deviation over 10 measurements.[44] The discrepancy with the timescale obtained for the anti-bunching profiles under CW operation $\tau_{\perp} \sim \tau_{HBT} \sim 3.5$ ns can be ascribed to the dependency of τ_{HBT} on both the excited state
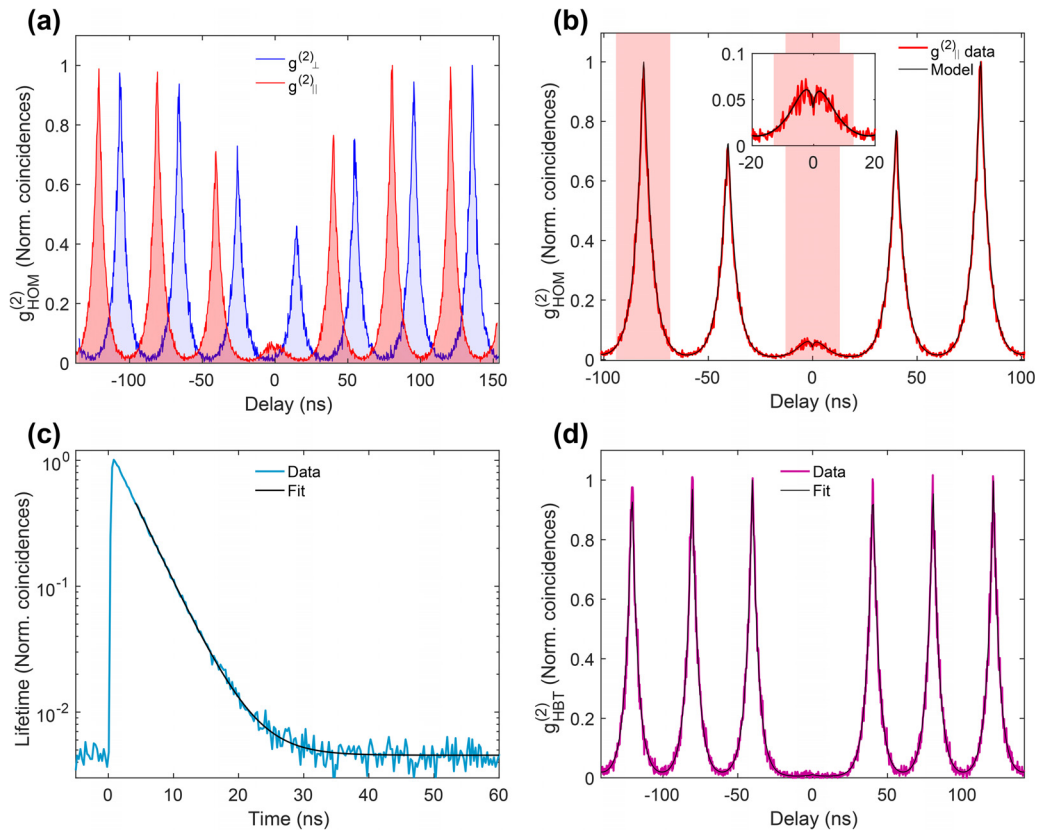
FIG. 2. Characterization of the source under pulsed excitation. (a) Histogram of the relative arrival time for HOM setup in the case of parallel (red) and orthogonal (blue) polarization of the input modes. The latter is shifted in time for clarity. (b) Zoom around zero time delay for parallel polarization. The shaded areas represent the 26 ns-wide time intervals considered for the visibility assessment. (c) Lifetime measurement and (d) histogram approximating the $g^{(2)}(\tau)$ in the HBT configuration. Black solid lines in (b)–(d) are fits to the data according to the equation in the main text. (a), (b), and (d) are obtained integrating 26 kcps on each SPAD for 45 and 15 min, respectively (normalization level corresponding to 925 and 292 coincidences; binning size 256 ps).

lifetime and pumping rate (see[29] the supplementary material). In order to perform HOM interference, the MZI delay and the temporal distance among neighboring pulses have to coincide. To this aim, the repetition rate is adjusted according to the result for Δt from the HOM fit in CW. The uncertainty associated with this measurement is estimated from the error in the fit parameter and amounts to about 200 ps. This directly impacts the uncertainty on the visibility, as it will be shown later. In Fig. 2(a), the $g^{(2)}_{HOM}(\tau)$ under pulsed excitation is compared for parallel and orthogonal polarization in red and blue solid lines, respectively, with the second one artificially delayed for sake of clarity. All curves are normalized with respect to the maximum peak amplitude, calculated averaging over more than ten pulses, excluding the ones in zero and $\pm \Delta t$. The latter pulses are associated with coincidences between photons that are one or two periods apart, leading to areas $A_{k=-1} = N(1 - R^2)$, $A_{k=+1} = N(1 - T^2)$, whereas all other peaks can be due to 3 classes of events, which sum up to a constant probability, $A_{k \leq -2} = A_{k \geq 2} = N$, with N being proportional to the integration time (supplementary material Ref. 45).

One way of defining the TPI visibility is through the comparison of the peak area around zero delay for the case of indistinguishable vs distinguishable photons, calculating the ratio, $V = \frac{A_\perp - A_\parallel}{A_\perp}$. In our case, integrating within a time window $\Delta T = 26$ ns (corresponding to about 96% of the photon wave packet area), we estimate a visibility $V = 78\% \pm 4\%$.[46] The results are further analyzed with a model based on Ref. 47, extrapolated for a train of infinite pulses (for details see the supplementary material), with the introduction of a phenomenological parameter v. This factor takes into account a non-perfect spatial alignment and polarization control, the residual multiphoton probability, as well as the effect of emission of distinguishable photons within the filter range but outside the ZPL. It amounts to the visibility that would be measured in the limit of negligible dephasing. As it can be appreciated in Fig. 2(b), the model correctly describes the data, considering the unbalance between $|r|^2$ and $|t|^2$ of the second beam splitter, the temporal resolution of the electronic system (230 ps, obtained as standard deviation of the $g^{(2)}_{HBT}(\tau)$ for laser pulses, details in the supplementary material) and a delay given by the inverse of the laser nominal repetition rate (24.79 MHz). The only free parameters in the model are the excited state lifetime τ_1, the pure dephasing Γ^* and v. A least squares fitting algorithm yields the following values:
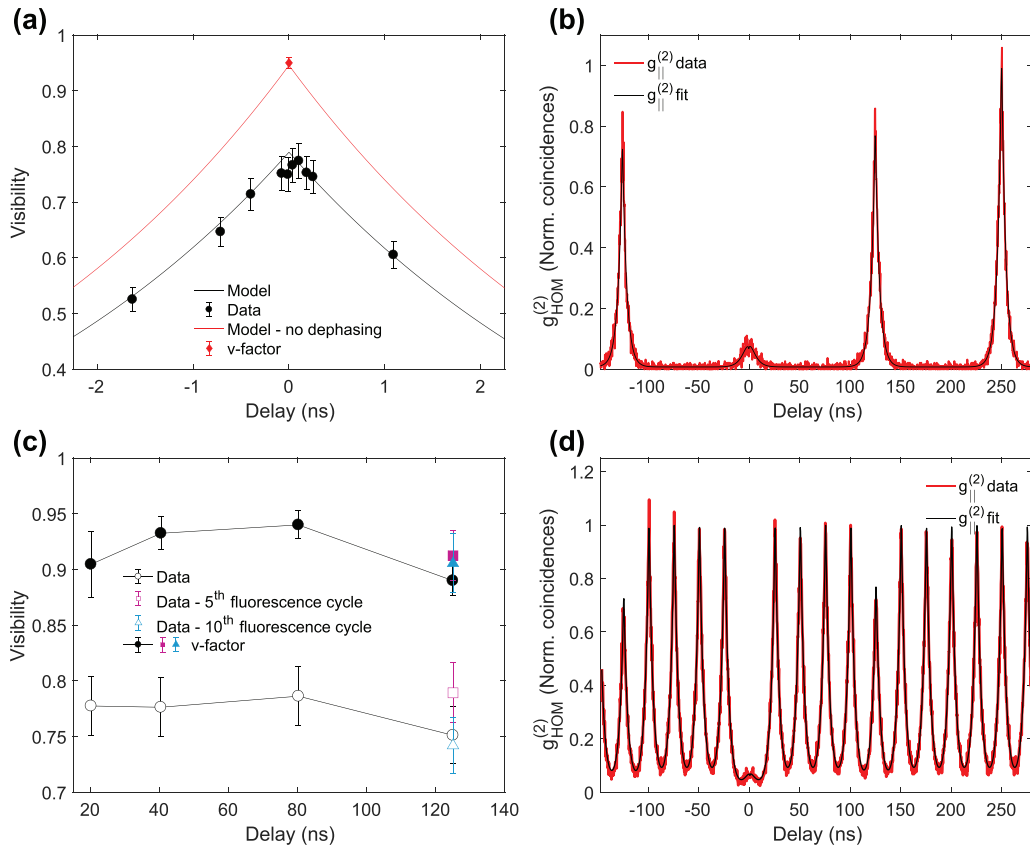
FIG. 3. HOM visibility under pulsed operation. (a) Visibility and *v*-factor as a function of the laser repetition rate. The delay is actually obtained varying the laser repetition rate, which determines the temporal overlap between the photon wave packets. (b) Coincidences histogram for 125 ns-long (25 m) delay line and parallel polarization. (c) Optimal HOM visibility and *v*-factor vs delay line length; for longest delay (125 ns), also the visibility of the interference between photons separated by multiple fluorescence cycles is reported as colored dots. (d) Coincidences histogram for 15 ns-long delay line and parallel polarization, in the case of 40 MHz repetition rate (interference between photons separated by five fluorescence cycles).

$\tau_1 = 4.04 \pm 0.02$ ns, $\Gamma^* = 55 \pm 10$ MHz, and $v = 0.95 \pm 0.02$. The first two parameters allow an independent estimation of the linewidth as $FWHM = \Gamma/\pi = 1/(2\pi\tau_1) + \Gamma^*/\pi = 57 \pm 4$ MHz, in substantial agreement with the direct measurement reported above.

Interestingly, the factor v is the visibility that could be obtained just cooling the system further to 1.4 K,[48] in order to get truly lifetime-limited linewidths ($FWHM = 1/(2\pi\tau_1) \simeq 40$ MHz). It is, therefore, important to understand what is limiting v to a value smaller than 1. Although the polarization optics have been characterized with an extinction ratio of 1/1600, the experimenter introduces an error in setting the relative orientation between the two arms. Another contribution could stem from the not-perfect purity of the single photon Fock state. This can be inferred from a measurement of the $g_{HBT}^{(2)}(\tau)$ in the HBT, reported, e.g., in Fig. 2(d), yielding $\tilde{g}_{HBT}^{(2)}(0) = A_0/A_N = 0.008 \pm 0.008$. Based on Ref. 49, we then estimate the mean wave packet overlap of the single photon component M_S, in the case of negligible dephasing and assuming full distinguishability for the rest of the input state,[49] as $M_S = \frac{v+1}{4RT(1-\tilde{g}^{(2)}(0))} - 1 \simeq 97\%$. Such value obviously depends on the filtering efficiency. In fact, the presence of a residual

component of distinguishable photons $(1 - \alpha)$, given by the portion of the emission in the PSB leaking through the notch filter, degrades the expected maximum visibility to[50] α^2. According to the fluorescence spectrum measured before and after the filter (reported in the supplementary material), roughly 98% of the light overlaps with the ZPL. In the optimal condition of zero dephasing but with the same filtering window, one can hence expect a visibility of 96%, which is just what has been estimated above.

Scanning the laser repetition rate and hence effectively the delay between the two photon wave packets, different sets of data are recorded, and the corresponding values for the visibility are plotted in Fig. 3(a), together with the derived theoretical curve. Using our model to estimate the error on the visibility, we observe that the main contribution to its uncertainty is given by the error in estimating the delay line (± 0.2 ns), that determines an uncertainty on V equal to about 4%. TPI has been measured also as a function of the delay in the unbalanced MZI and the distance among interfering particles in number of photons. In Fig. 3(b), the $g_{HOM}^{(2)}(\tau)$ using parallel polarizations for a delay of 125.0 ± 0.2 ns (around 25 m) is reported. It is worth noticing that the visibility starts to decrease only around such time

delay [see Fig. 3(c)], which corresponds to about 30 times the photon wave packet extension. Remarkably, as reported in the visibility graph in Fig. 3(c), we observe no relevant drop in TPI also between photons separated by up to 10 fluorescence cycles. As an example, Fig. 3(d) shows the coincidences histogram for the case of interference between photons separated by five fluorescence cycles. Here a delay Δt of 125 ns was employed with a laser repetition rate of 40 MHz. Such a remarkable spectral stability is in agreement with the negligible spectral diffusion reported for CW operation both here and in the literature.[38,39]

In conclusion, in this paper we demonstrate triggered generation of highly indistinguishable single photons from a single organic dye molecule under non-resonant pulsed excitation. The results are obtained for emitters in a sub-micrometric environment, without the help of any photonic resonance, and using only a 0.4 nm-wide spectral filter to select the emission. A HOM interference visibility of more than 75% is reported, limited by the residual dephasing present at the operating temperature of 3 K. A visibility of 96% is expected for the very same experiment in the case of 1.5 kelvin operation. We also find that HOM visibility does not show relevant reduction for photons separated by up to 125 ns (equivalent to 30 times the wave packet duration) and by up to 10 fluorescence cycles. Such a spectral stability is of major interest for applications involving multiple photons, such as linear optical quantum computing, where temporal demultiplexing is a typical strategy to increase the number of available resources. The source presented in this paper shows a brightness at detector limited to around 2%, corresponding to a brightness at first lens (N.A. = 0.67) of around 5%. Hence, in the perspective of implementation for quantum applications, integration of the emitter with photonic devices becomes mandatory. A photonic resonance can modify both the radiation pattern and the spectral distribution of the emission, in order to bring the source brightness to the state-of-the-art level.[51] In this respect, the same type of system has been shown to be particularly suitable for the integration in hybrid photonic structures.[52,53]

See the supplementary material that contains (i) theoretical calculation of the function used to fit the coincidences histograms under pulsed operation; (ii) calibration of the response function of the electronic chain for the collection of the coincidences histograms; (iii) emission spectrum of the molecule under investigation and considerations concerning PSB contribution in the photon stream selected by the Notch filter.

AUTHORS' CONTRIBUTIONS

P.L. and C.T. conceived the research and designed the experiments. All authors performed the experiments; R.D. developed the theoretical model and performed data analysis under the supervision of C.T.; P.L., M.C., and C.T. wrote the manuscript with critical feedback from all authors.

The authors declare no conflicts of interest.

DATA AVAILABILITY

The data that support the findings of this study are available from the corresponding author upon reasonable request.

REFERENCES

[1]I. Abram, R. Raj, J.-L. Oudar, and G. Dolique, "Direct observation of the second-order coherence of parametrically generated light," Phys. Rev. Lett. **57**, 2516 (1986).

[2]C. K. Hong, Z. Y. Ou, and L. Mandel, "Measurement of subpicosecond time intervals between two photons by interference," Phys. Rev. Lett. **59**, 2044–2046 (1987).

[3]Y. Shih and C. O. Alley, "New type of Einstein-Podolsky-Rosen-Bohm experiment using pairs of light quanta produced by optical parametric down-conversion," Phys. Rev. Lett. **61**, 2921 (1988).

[4]J. G. Rarity and P. Tapster, "Fourth-order interference in parametric down-conversion," J. Opt. Soc. Am. B **6**, 1221–1226 (1989).

[5]R. Liu, B. Odom, Y. Yamamoto, and S. Tarucha, "Quantum interference in electron collision," Nature **391**, 263–265 (1998).

[6]I. Neder, N. Ofek, Y. Chung, M. Heiblum, D. Mahalu, and V. Umansky, "Interference between two indistinguishable electrons from independent sources," Nature **448**, 333–337 (2007).

[7]R. W. Heeres, L. P. Kouwenhoven, and V. Zwiller, "Quantum interference in plasmonic circuits," Nat. Nanotechnol. **8**, 719–722 (2013).

[8]J. S. Fakonas, H. Lee, Y. A. Kelaita, and H. A. Atwater, "Two-plasmon quantum interference," Nat. Photonics **8**, 317–320 (2014).

[9]A. Kaufman, B. Lester, C. Reynolds, M. Wall, M. Foss-Feig, K. Hazzard, A. Rey, and C. Regal, "Two-particle quantum interference in tunnel-coupled optical tweezers," Science **345**, 306–309 (2014).

[10]R. Lopes, A. Imanaliev, A. Aspect, M. Cheneau, D. Boiron, and C. I. Westbrook, "Atomic Hong-Ou–Mandel experiment," Nature **520**, 66–68 (2015).

[11]R. J. Glauber, "One hundred years of light quanta (Nobel Lecture)," ChemPhysChem **7**, 1618–1639 (2006).

[12]H. Paul, "Interference between independent photons," Rev. Mod. Phys. **58**, 209 (1986).

[13]F. Bouchard, A. Sit, Y. Zhang, R. Fickler, F. M. Miatto, Y. Yao, F. Sciarrino, and E. Karimi, "Two-photon interference: The Hong-Ou-Mandel effect," Rep. Prog. Phys. **84**, 012402 (2021).

[14]E. Knill, R. Laflamme, and G. J. Milburn, "A scheme for efficient quantum computation with linear optics," Nature **409**, 46–52 (2001).

[15]J. L. O'Brien, "Optical quantum computing," Science **318**, 1567–1570 (2007).

[16]N. Sangouard, C. Simon, H. de Riedmatten, and N. Gisin, "Quantum repeaters based on atomic ensembles and linear optics," Rev. Mod. Phys. **83**, 33–80 (2011).

[17]C. Sparrow, E. Martín-López, N. Maraviglia, A. Neville, C. Harrold, J. Carolan, Y. N. Joglekar, T. Hashimoto, N. Matsuda, J. L. O' Brien, D. P. Tew, and A. Laing, "Simulating the vibrational quantum dynamics of molecules using photonics," Nature **557**, 660–667 (2018).

[18]F. J. García de Abajo and A. Howie, "Retarded field calculation of electron energy loss in inhomogeneous dielectrics," Phys. Rev. B **65**, 115418 (2002).

[19]D. G. Angelakis, "Quantum simulations with photons and polaritons," in *Quantum Science and Technology* (Springer, 2017), p. 134.

[20]J. P. Dowling, "Quantum optical metrology–the lowdown on high-N00N states," Contemp. Phys. **49**, 125–143 (2008).

[21]V. Giovannetti, S. Lloyd, and L. Maccone, "Advances in quantum metrology," Nat. Photonics **5**, 222–229 (2011).

[22]A. Lyons, G. C. Knee, E. Bolduc, T. Roger, J. Leach, E. M. Gauger, and D. Faccio, "Attosecond-resolution Hong–Ou–Mandel interferometry," Sci. Adv. **4**, eaap9416 (2018).

[23]The N = 2 NOON state with + sign is obtained in the specific case of a beam splitter which is symmetric in the phase accumulated under reflection from both sides.

[24]I. Aharonovich, D. Englund, and M. Toth, "Solid-state single-photon emitters," Nat. Photonics **10**, 631–641 (2016).

[25] J.-P. Li, J. Qin, A. Chen, Z.-C. Duan, Y. Yu, Y. Huo, S. Höfling, C.-Y. Lu, K. Chen, and J.-W. Pan, "Multiphoton graph states from a solid-state single-photon source," ACS Photonics **7**, 1603–1610 (2020).

[26] D. Istrati, Y. Pilnyak, J. C. Loredo, C. Antón, N. Somaschi, P. Hilaire, H. Ollivier, M. Esmann, L. Cohen, L. Vidro, C. Millet, A. Lemaitre, I. Sagnes, A. Harouri, L. Lanco, P. Senellart, and H. S. Eisenberg, "Sequential generation of linear cluster states from a single photon emitter," Nat. Commun. **11**, 5501 (2020).

[27] J. Liu, K. Konthasinghe, M. Davanço, J. Lawall, V. Anant, V. Verma, R. Mirin, S. W. Nam, J. D. Song, B. Ma, Z. S. Chen, H. Q. Ni, Z. C. Niu, and K. Srinivasan, "Single self-assembled InAs/GaAs quantum dots in photonic nanostructures: The role of nanofabrication," Phys. Rev. Appl. **9**, 064019 (2018).

[28] U. Jantzen, A. B. Kurz, D. S. Rudnicki, C. Schäfermeier, K. D. Jahnke, U. L. Andersen, V. A. Davydov, V. N. Agafonov, A. Kubanek, L. J. Rogers, and F. Jelezko, "Nanodiamonds carrying silicon-vacancy quantum emitters with almost lifetime-limited linewidths," New J. Phys. **18**, 073036 (2016).

[29] K. Lee, X.-W. Chen, H. Eghlidi, P. Kukura, R. Lettow, A. Renn, V. Sandoghdar, and S. Götzinger, "A planar dielectric antenna for directional single-photon emission and near-unity collection efficiency," Nat. Photonics **5**, 166–169 (2011).

[30] D. Wang, H. Kelkar, D. Martin-Cano, D. Rattenbacher, A. Shkarin, T. Utikal, S. Götzinger, and V. Sandoghdar, "Turning a molecule into a coherent two-level quantum system," Nat. Phys. **15**, 483–489 (2019).

[31] P. Lombardi, A. P. Ovvyan, S. Pazzagli, G. Mazzamuto, G. Kewes, O. Neitzke, N. Gruhler, O. Benson, W. H. P. Pernice, F. S. Cataliotti, and C. Toninelli, "Photostable molecules on chip: Integrated sources of nonclassical light," ACS Photonics **5**(1), 126–132 (2018).

[32] D. Rattenbacher, A. Shkarin, J. Renger, T. Utikal, S. Götzinger, and V. Sandoghdar, "Coherent coupling of single molecules to on-chip ring resonators," New J. Phys. **21**, 062002 (2019).

[33] C. Toninelli, I. Gerhardt, A. S. Clark, A. Reserbat-Plantey, S. Götzinger, Z. Ristanovic, M. Colautti, P. Lombardi, K. D. Major, I. Deperasińska, W. H. Pernice, F. H. L. Koppens, B. Kozankiewicz, A. Gourdon, V. Sandoghdar, and M. Orrit, "Single organic molecules for photonic quantum technologies," Nat. Mater. (published online 2021).

[34] A. Kiraz, M. Ehrl, T. Hellerer, O. E. Müstecaplıoğlu, C. Bräuchle, and A. Zumbusch, "Indistinguishable photons from a single molecule," Phys. Rev. Lett. **94**, 223602 (2005).

[35] J.-B. Trebbia, P. Tamarat, and B. Lounis, "Indistinguishable near-infrared single photons from an individual organic molecule," Phys. Rev. A **82**, 063803 (2010).

[36] M. Rezai, J. Wrachtrup, and I. Gerhardt, "Coherence properties of molecular single photons for quantum networks," Phys. Rev. X **8**, 031026 (2018).

[37] M. Rezai, J. Wrachtrup, and I. Gerhardt, "Polarization-entangled photon pairs from a single molecule," Optica **6**, 34–40 (2019).

[38] R. Lettow, Y. L. A. Rezus, A. Renn, G. Zumofen, E. Ikonen, S. Götzinger, S. zinger, and V. Sandoghdar, "Quantum interference of tunably indistinguishable photons from remote organic molecules," Phys. Rev. Lett. **104**, 123605 (2010).

[39] S. Pazzagli, P. Lombardi, D. Martella, M. Colautti, B. Tiribilli, F. S. Cataliotti, and C. Toninelli, "Self-assembled nanocrystals of polycyclic aromatic hydrocarbons show photostable single-photon emission," ACS Nano **12**, 4295–4303 (2018).

[40] P. Lombardi, M. Trapuzzano, M. Colautti, G. Margheri, I. P. Degiovanni, M. López, S. Kück, and C. Toninelli, "A molecule-based single-photon source applied in quantum radiometry," Adv. Quantum Technol. **3**, 1900083 (2020).

[41] S. Checcucci, P. Lombardi, S. Rizvi, F. Sgrignuoli, N. Gruhler, F. B. Dieleman, F. S. Cataliotti, W. H. Pernice, M. Agio, and C. Toninelli, "Beaming light from a quantum emitter with a planar optical antenna," Light **6**, e16245 (2017).

[42] R. H. Brown and R. Q. Twiss, "Correlation between photons in two coherent beams of light," Nature **177**, 27–29 (1956).

[43] R. B. Patel, A. J. Bennett, K. Cooper, P. Atkinson, C. A. Nicoll, D. A. Ritchie, and A. J. Shields, "Postselective two-photon interference from a continuous nonclassical stream of photons emitted by a quantum dot," Phys. Rev. Lett. **100**, 207405 (2008).

[44] In this case we can approximate the population relaxation time just with its radiative component, based on the characteristic molecule off-times in the triplet state, discussed, e.g., in Ref. 48.

[45] J. C. Loredo, N. A. Zakaria, N. Somaschi, C. Anton, L. de Santis, V. Giesz, T. Grange, M. A. Broome, O. Gazzano, G. Coppola, I. Sagnes, A. Lemaitre, A. Auffeves, P. Senellart, M. P. Almeida, and A. G. White, "Scalable performance in solid-state single-photon sources," Optica **3**, 433–440 (2016).

[46] Increasing the integration time to the entire period, the corresponding visibility would decrease to 76%. For the purpose of limiting the influence of the background and of signal due to neighboring peaks in the visibility estimation, we always consider an integration window of ±13 ns, that is anyway more than three times longer than the excited state lifetime.

[47] B. Kambs and C. Becher, "Limitations on the indistinguishability of photons from remote solid state sources," New J. Phys. **20**, 115003 (2018).

[48] A. A. L. Nicolet, C. Hofmann, M. A. Kol'chenko, B. Kozankiewicz, and M. Orrit, "Single dibenzoterrylene molecules in an anthracene crystal: Spectroscopy and photophysics," ChemPhysChem **8**, 1215–1220 (2007).

[49] H. Ollivier, S. E. Thomas, S. C. Wein, I. M. de Buy Wenniger, N. Coste, J. C. Loredo, N. Somaschi, A. Harouri, A. Lemaitre, I. Sagnes, L. Lanco, C. Simon, C. Anton, O. Krebs, and P. Senellart, "Hong–Ou–Mandel interference with imperfect single photon sources," Phys. Rev. Lett. **126**, 063602 (2021).

[50] C. Clear, R. C. Schofield, K. D. Major, J. Iles-Smith, A. S. Clark, and D. P. S. McCutcheon, "Phonon-induced optical dephasing in single organic molecules," Phys. Rev. Lett. **124**, 153602 (2020).

[51] H. Wang, Y.-M. He, T.-H. Chung, H. Hu, Y. Yu, S. Chen, X. Ding, M.-C. Chen, J. Qin, X. Yang et al., "Towards optimal single-photon sources from polarized microcavities," Nat. Photonics **13**, 770–775 (2019).

[52] M. Colautti, P. Lombardi, M. Trapuzzano, F. S. Piccioli, S. Pazzagli, B. Tiribilli, S. Nocentini, F. S. Cataliotti, D. S. Wiersma, and C. Toninelli, "A 3D polymeric platform for photonic quantum technologies," Adv. Quantum Technol. **3**, 2000004 (2020).

[53] P. Lombardi, A. P. Ovvyan, S. Pazzagli, G. Mazzamuto, G. Kewes, O. Neitzke, N. Gruhler, O. Benson, W. H. P. Pernice, F. S. Cataliotti, and C. Toninelli, "Photostable molecules on chip: Integrated sources of nonclassical light," ACS Photonics **5**, 126 (2018).